

Error Performance for MC-CDMA and OFDMA in a Downlink Multi-Cell Scenario

Simon Plass¹, Armin Dammann¹, and Stefan Kaiser²

¹ German Aerospace Center (DLR), Institute of Communications and Navigation, Oberpfaffenhofen, 82234 Wessling, Germany, {simon.plass, armin.dammann}@dlr.de

² DoCoMo Communications Laboratories Europe GmbH, Landsbergerstr. 312, 80687 Munich, Germany, kaiser@docomolab-euro.com

Abstract—This paper studies the error performances of two different 4G downlinks in a multi-cell environment. On the one hand, an orthogonal frequency division multiplexing (OFDM) based multiple access scheme (OFDMA), and on the other hand, a multi-carrier code division multiple access (MC-CDMA) scheme is proposed. Both transmission schemes are implemented in a cellular structure. The cellular environment model takes into account path loss and shadowing depending on the position of the mobile terminal. Further investigations are done by introducing a radio resource management (RRM) for OFDMA which can improve the performance for lower system loads. Error performances are given to compare the two multiple access proposals. The results show that MC-CDMA outperforms OFDMA in the inner part of the cell for lower resource loads by utilizing its whole diversity of used sub-carriers. At the edge of the cell, the RRM can highly enhance the OFDMA performance mainly for low resource loads and OFDMA surpasses the MC-CDMA performance.

I. INTRODUCTION

For 4G systems several proposals of transmission schemes have been made [1], [2], [3] and are based on orthogonal frequency division multiplexing (OFDM) [4]. A major benefit of OFDM is the robustness against multipath propagation channels, and therefore, high data rate transmissions are possible. The assignment of one or several sub-carriers to each user in an OFDM system leads to the multiple access scheme OFDMA. Contrary to OFDMA, the multi-carrier code division multiple access (MC-CDMA) scheme transmits in parallel chips of a spread data symbol on different sub-carriers [1]. In OFDMA user-data symbols are allocated directly to channel resources and therefore offers no diversity without channel coding but adaptive transmission is possible. In contrast, an MC-CDMA transmission scheme spreads the user-data symbol energy over all channel resources and therefore offers diversity. However, MC-CDMA suffers from multiple access interference (MAI) due to the deorthogonalization of the spreading codes.

Over the last decade, such downlink systems have been studied intensively. However, it is necessary to extend the investigations to more realistic scenarios, *i.e.*, cellular structures. Since each user allocates its own sub-carriers in an OFDMA system, a radio resource management (RRM) can be introduced for a cellular environment.

The goal of this paper is the investigation and discussion of the two technologies in anticipation of 4G requirements

regarding the error performances.

The remaining parts of this paper are organized as follows. The next section introduces the used multi-carrier systems, including the transmitter, receiver, and assumed channel model. Section III describes in more detail the model for the different propagation impairments affecting the cellular system and the used RRM for OFDMA. The cellular interference modeling is in the focus of Section III-B. Finally, Section IV presents error performances for the used transmission schemes in a multi-cell environment.

II. MULTI-CARRIER SYSTEMS

The transmitter and receiver of an OFDMA and MC-CDMA transmission scheme differ only in the sub-carrier allocation and the additional spreading and detection component for MC-CDMA. In this paper, the terminology, notation, and description is identical for both systems, and the differences are pointed out in this section.

The block diagram of a transmitter using OFDMA/MC-CDMA is shown in Figure 1. The information bit stream of the N_u active users are convolutionally encoded and interleaved by the outer interleaver Π_{out} . With respect to the modulation alphabet, the bits are mapped to complex-valued data symbols. In the sub-carrier allocation block N_d symbols per user are arranged for each transmission scheme. In the case of MC-CDMA, the k th data symbol is multiplied by a user-specific Walsh-Hadamard spreading sequence which provides so-called chips. The spreading length L corresponds to the maximum number of active user $L = N_{u,\text{max}}$.

An inner sub-carrier interleaver Π_{in} allows a better exploitation of diversity. The input block of the interleaver is denoted as one OFDM symbol and N_s OFDM symbols describe one OFDM frame. A one-dimensional (1D) interleaving in frequency direction is possible, and by taking into account a whole OFDM frame, a two-dimensional (2D) interleaving in frequency and time direction is also applicable [5]. These methods can also be referred to as frequency or time/frequency hopping. The latter introduces an additional TDMA component.

Finally, an OFDM modulation is performed which includes an inverse fast Fourier transformation (IFFT) with a FFT length of N_{FFT} and insertion of a guard interval to avoid inter-symbol and inter-carrier interference.

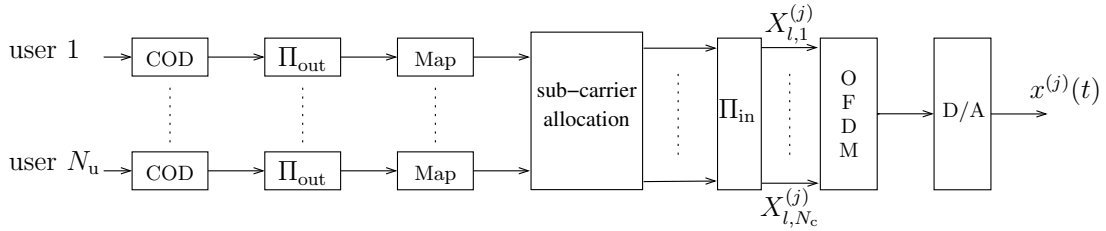


Fig. 1. OFDMA/MC-CDMA transmitter of the j th base station

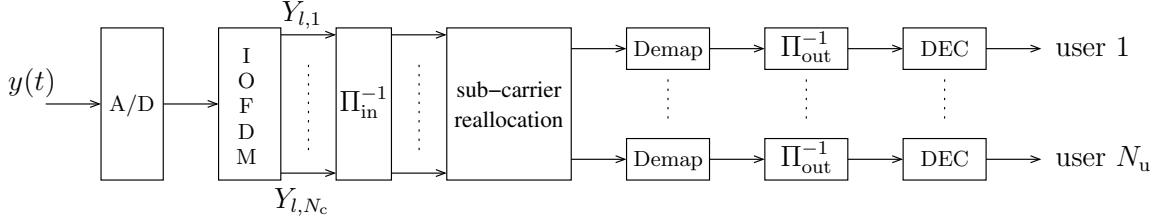


Fig. 2. OFDMA/MC-CDMA receiver

On the receiver side, see Figure 2, the transmitter signal processing is inverted.

In MC-CDMA the distortion due to the flat fading on each sub-channel is compensated by equalization. The received chips are equalized by using a linear minimum mean square error (MMSE) one-tap equalizer. The resulting MMSE equalizer coefficients are

$$G_{l,i} = \frac{H_{l,i}^{(j)*}}{|H_{l,i}^{(j)}|^2 + \frac{L}{N_u}\sigma^2} \quad i = 1, \dots, N_c, \quad (1)$$

where σ^2 is the actual variance of additive white Gaussian noise (AWGN) process and $H_{l,i}^{(j)}$ is the channel transfer function (CTF) from base station (BS) j to the mobile terminal (MT). Furthermore, N_c is the number of sub-carriers and the indices j and i represent the OFDM symbol and sub-carrier, respectively. In contrast, for OFDMA the data symbols are directly demodulated with the knowledge of $H_{l,i}^{(j)}$.

Then, the symbol demapper maps the data symbols to bits. In addition, it calculates the log-likelihood ratio for each bit based on the selected alphabet. The code bits are deinterleaved and finally decoded using soft-decision Viterbi decoding [1].

For the multi-carrier schemes a resource load (RL) can be defined. For the OFDMA system, the RL is the ratio of the number of assigned sub-carriers to the total number of available sub-carriers N_c . This corresponds directly to the RL of the MC-CDMA system, which is defined by the ratio of the number of active users to the number of maximum users. Note that in terms of total transmitted signal energy, the following relation holds.

$$\text{RL} = \text{RL}_{\text{OFDMA}} = \frac{N_d N_u}{N_c} = \text{RL}_{\text{MC-CDMA}} = \frac{N_u}{L} \quad (2)$$

A. Channel Model

The mobile radio channel is assumed to be a time-variant, frequency-selective fading channel. It is modeled by a tapped delay-line with Q_0 non-zero taps [6]. We consider that the Q_0 channel taps are mutually uncorrelated and all tap delays $\tau_q^{(j)}$ are in the range $[0, \tau_{\max}]$. The channel fading is assumed to

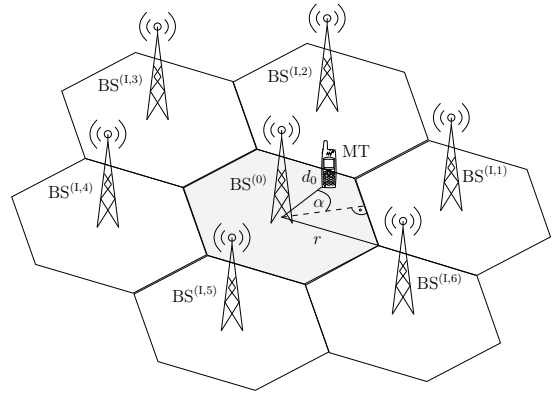


Fig. 3. One-tier multi-cell environment

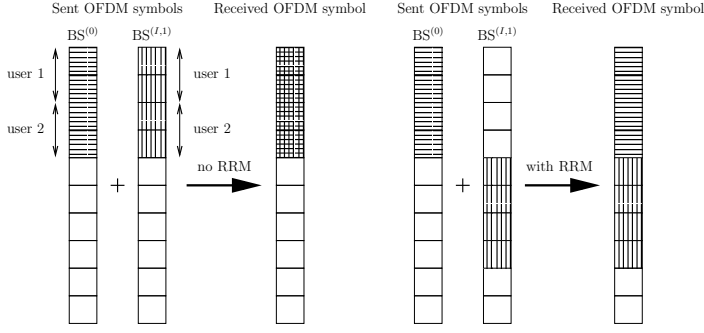
be a wide-sense stationary uncorrelated scattering (WSSUS) random process, *i.e.*, the channel has a fading statistic that remains constant over a period of time [7]. The CTF in (1) is the Fourier transform of the channel impulse response defined by

$$H_{l,i}^{(j)} = \sum_{q=1}^{Q_0} h_{l,q}^{(j)} e^{-j2\pi\tau_q^{(j)}i/T_s}, \quad (3)$$

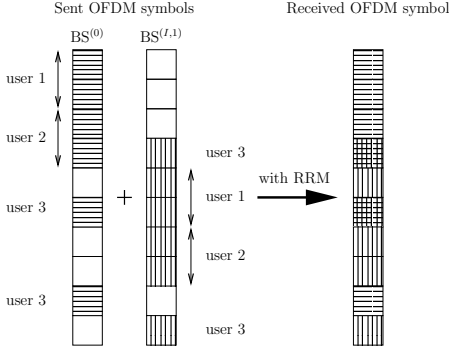
where $T_s = N_{\text{FFT}}T_{\text{samp}}$ is the OFDM symbol duration without the guard interval and T_{samp} is the sampling duration.

III. MULTI-CELL ENVIRONMENT

A typical hexagonal structure is assumed for the cellular network where all cell sizes are equal as depicted in Figure 3. A whole tier of interfering cells around the desired cell is assumed. The BS and the mobile terminal (MT) are perfectly synchronized in time and frequency. The distance between the desired BS and MT is denoted as d_0 , and the cell radius r is normalized to 1. For example, the mobile can be situated along a line from the desired BS to the intersection of the desired cell and two interfering cells. In this case, the angle $\alpha = 30^\circ$. A propagation model represents the locally averaged received energy from the j th BS at the MT. The slowly varying signal energy attenuation due to path loss is generally modeled as



(a) Received symbol of 2 active users per BS



(b) Received symbol of 3 active users per BS

Fig. 4. Radio resource management with $m_{\text{RRM}} = 2$

the product of the γ th power of distance d_j and a log-normal component representing shadowing losses [8]. Therefore the resulting received signal energy is

$$E_j = E_{t,j} \cdot d_j^{-\gamma} \cdot 10^{\eta_j/10\text{dB}}, \quad (4)$$

where $E_{t,j}$ is the transmitted signal energy from the j th BS. The path decay factor γ is assumed to be 4 and the standard deviation of the Gaussian-distributed shadowing factor η_j is set to 8 dB. The cellular simulation environment is taken from [9].

A. Radio Resource Management for OFDMA

Introduction of a radio resource management for assigning sub-carriers should maximize the performance in the case of OFDMA. This management process is illustrated in Figure 4. In a fully-synchronized system, it is possible to assign the sub-carriers per BS in such a way that no double allocation of sub-carriers between the BSs occurs. This can be guaranteed up to a resource load of $\text{RL} = 1/m_{\text{RRM}}$, where m_{RRM} is the total number of managed cells. The managed m_{RRM} BSs need the same inner interleaver Π_{in} after the sub-carrier allocation. In spite of RRM the frequency diversity of the OFDMA system is preserved. The unmanaged cells use their own independent inner interleaver. See Figure 4(a) as an example of transmitted OFDM symbols of two unmanaged BSs and two managed ones. By exceeding this RL, the succeeding assignment of sub-carriers is done in such a way that the assigned sub-carriers per additional active user are randomly distributed over the remaining sub-carriers. This is shown for user 3 in Figure 4(b).

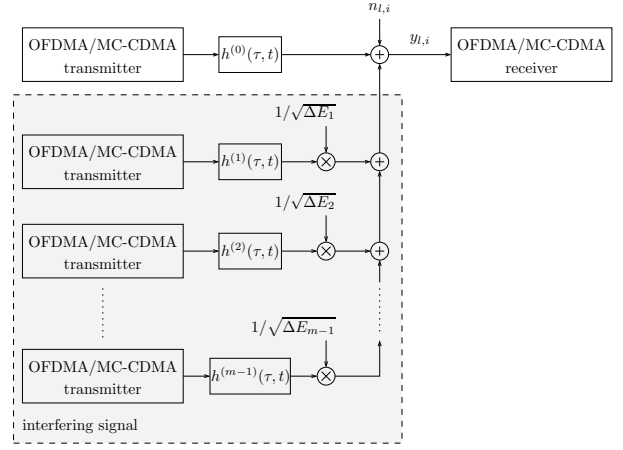


Fig. 5. Model of the cellular system

Therefore, the probability that any user is entirely disturbed is reduced.

B. Cellular Interference Modeling

The cellular interference can be modeled as depicted in Figure 5. The channels have the same Doppler power spectrum and delay profile, but are uncorrelated. The ratio of the received signal energy from the desired BS and from an interfering BS j is denoted by $\Delta E_j = E_0/E_j$. Therefore, the interfering signals from BS^(l,j) are weighted with the energy factor $1/\sqrt{\Delta E_j}$.

By including the interfering BSs, the received l th OFDM symbol at sub-carrier i becomes

$$Y_{l,i} = X_{l,i}^{(0)} H_{l,i}^{(0)} + \sum_{j=1}^{m-1} \frac{1}{\sqrt{\Delta E_j}} X_{l,i}^{(j)} H_{l,i}^{(j)} + N_{l,i}, \quad (5)$$

where $X_{l,i}^{(j)}$ denotes the value of the i th sub-carrier in the l th OFDM symbol at BS j and $N_{l,i}$ is AWGN with zero mean and variance N_0 . This scenario represents a power-controlled desired user at distance d_0 as well as power-controlled interfering cells.

In the case of MC-CDMA, the signals are passed to a MMSE equalizer after the deinterleaving process in the receiver. The coefficients in (1) have to be modified in such a way that the interfering signals are assumed to be an additional noise variance term in the denominator [9].

IV. SIMULATION RESULTS

Table I illustrates the system parameters of the used transmission systems. The channel model as shown in Figure 6, see also Section II-A, is a tapped delay-line model with Q_0 taps, $\Delta\tau$ tap spacing, and an exponentially decaying power delay profile. Corresponding to a mobile velocity of about 3 km/h at 5 GHz carrier frequency, each tap has a normalized maximum Doppler frequency $f_{\text{Dnorm,max}} = f_{\text{D,max}} \cdot T_s = 14 \text{ Hz} \cdot 7.5 \mu\text{s} = 10^{-4}$, where T_s represents the OFDM symbol duration. These parameters are taken from [10]. Quadrature phase shift keying (QPSK) is used for both systems. In addition, perfect channel knowledge is assumed. Consequently, the CTF in (3) is known at the receiver. Furthermore, a

TABLE I
PARAMETERS OF THE TRANSMISSION SYSTEMS

Bandwidth	B	101.25 MHz
# sub-carriers	N_c	768
FFT length	N_{FFT}	1024
Guard interval length	N_{GI}	226
Sample duration	T_{samp}	7.4 ns
Frame length	N_{frame}	64
# active users	N_u	$\{1 \dots 8\}$
Spreading length (MC-CDMA)	L	8
Modulation		QPSK
Channel coding		CC (171, 133) _{oct}
Channel coding rate	R	1/2
Channel coding memory	M_{CC}	6

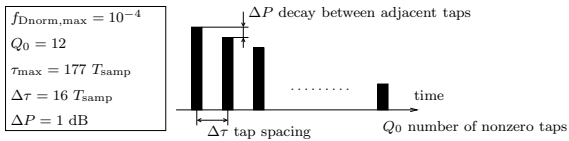


Fig. 6. Parameters of the used power delay profile of the channel model convolutional code (CC) with rate $R = 1/2$ and memory $M_{\text{CC}} = 6$ was selected as an outer channel code. Finally, the average energy per bit divided by the average noise power of AWGN is set to $E_b/N_0 = 10$ dB for all users in the simulations. In the case of MC-CDMA, the spreading length is set to $L = 8$.

For the following simulations, the interfering BSs have the identical parameters as the desired BS which also includes the number of active users. The MT moves from the BS in an angle of $\alpha = 30^\circ$. The statistics of the used distance dependent propagation model remain constant over the period of one OFDM frame. The two closest interfering BSs to the MT have the largest influence of disturbance in a multi-cell environment [5]. Therefore, in the case of RRM for OFDMA, the resources of the desired BS and the two closest interfering BSs are managed, see Section III-A. Note that the simulations are carried out with 2D inner interleavers Π_{in} and any variation is explicitly mentioned.

Figure 7 depicts the carrier-to-interference ratio (C/I) in dB versus the distance d_0 . Since the spreading combines the signals and all available sub-carriers are allocated, there is no difference in the C/I by varying the RL at d_0 for MC-CDMA. The C/I performance of a fully-loaded OFDMA scheme is equal to the MC-CDMA case because all sub-carriers are also allocated. For lower RLs in OFDMA and the use of randomly chosen 2D interleavers in each cell, there are less sub-carrier allocation collisions and the C/I increases. Furthermore, with the RRM the major disturbance of the closest interfering BS is avoided, and an additional C/I gain is possible.

The simulations in Figure 8 show a direct comparison between the two 4G proposals OFDMA and MC-CDMA in a cellular environment where the bit error rate (BER) versus the RL is presented. Since the number of active users, the maximum number of users, the data symbols per user, and the frame size are equal, the comparison of the systems is fair in

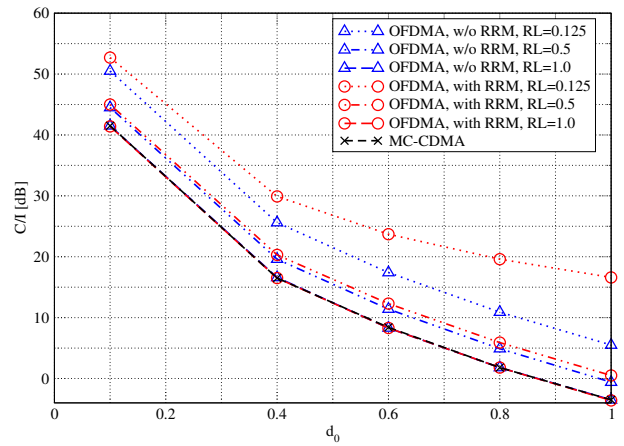


Fig. 7. Relationship between the C/I and the distance d_0

that case. Two scenarios are illustrated.

First scenario, $d_0 = 0.4$: Since the interference is negligible for $d_0 \leq 0.4$ [5], the RRM does not enhance the OFDMA performance. And in spite of the increasing C/I for lower RLs, the OFDMA performance keeps almost constant by increasing the RL in contrast to the performance of MC-CDMA. For small RLs, MC-CDMA outperforms OFDMA by far because MC-CDMA can utilize the whole diversity of all assigned sub-carriers. The benefit of MC-CDMA reduces with increasing RL because the multiple access interference (MAI) increases for higher RLs.

Second scenario, $d_0 = 1.0$: The MT is at the cell boundary, where two interfering BS are at the same distance as the desired BS. Thus, the cellular interference is maximal. Only in a small region of lower RLs MC-CDMA gains in comparison to OFDMA without RRM. At a RL of $3/8$, the performances merge and keep constant. OFDMA with RRM has a huge performance gain up to a RL = $3/8$. The RRM can avoid any collision with the major interfering signals from the neighboring cells up to a RL = $1/3$.

Similar to OFDMA [5], MC-CDMA benefits from the additional diversity in time direction. Figure 8 shows a performance loss by using a 1D interleaving, represented by the dashed-dotted line, instead of a 2D interleaving for the $d_0 = 0.4$ scenario. The additional diversity gain, due to 2D interleaving, is more significant when the MAI decreases for lower RLs. For higher RLs, the performances for 1D and 2D interleaving merge.

In [9] and [5], it was shown that in the peripheral area of the desired cell, a strong disturbance by the adjacent interfering cells exists. In contrast, the core of the desired cell ($d_0 \leq 0.4$) obtains a minimum of interference. Therefore, we see in Figure 8 a huge performance degradation between the two scenarios $d_0 = 0.4$ and $d_0 = 1.0$. In the same way, the performances of Figure 9 are influenced. The BER is plotted as a function of the distance d_0 for different transmission schemes in the same multi-cell environment. The performances show a distinctively steeper slope for $d_0 > 0.4$.

The performance for OFDMA with RRM and an RL = $1/8$ in Figure 9 keeps roughly constant because no sub-carriers are doubly allocated due to the RRM. A small performance

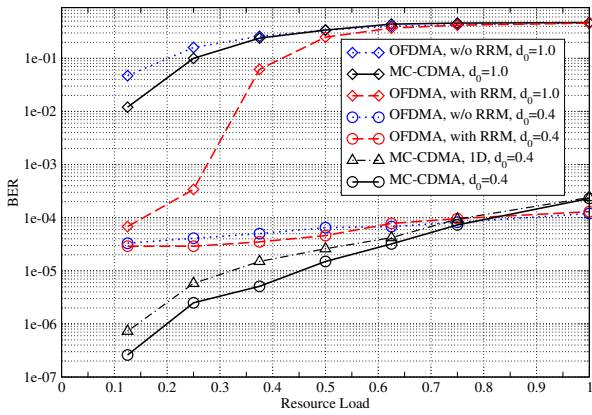


Fig. 8. BER versus resource load @ $E_b/N_0 = 10$ dB for an OFDMA and MC-CDMA system in a multi-cell environment and perfect channel estimation for two different d_0

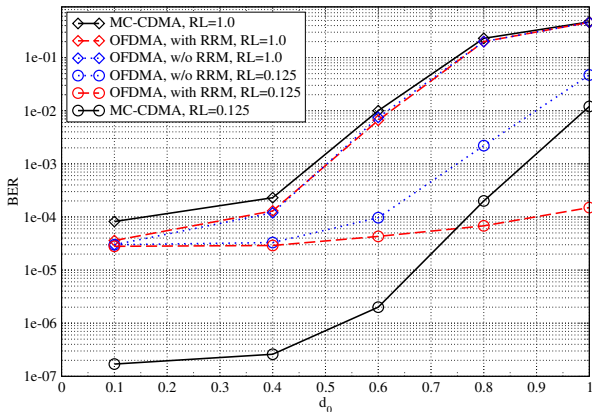


Fig. 9. BER versus d_0 @ $E_b/N_0 = 10$ dB for an OFDMA and MC-CDMA system in a multi-cell environment and perfect channel estimation for two different resource loads

loss exists, resulting from the higher inter-cell interference. Again, MC-CDMA outperforms OFDMA for $RL = 1/8$ in the inner cell area up to $d_0 = 0.75$. In contrast, OFDMA slightly exceeds the MC-CDMA performance in the fully-loaded scenario because the MAI is the major degradation factor of MC-CDMA. Since all sub-carriers are allocated in the fully-loaded case, there is no difference between OFDMA with RRM and without RRM.

For future 4G downlink transmission schemes, we propose a radial partitioned cell structure like onion rings. By allocating separated sub-carrier resources for OFDMA and MC-CDMA, a hybrid cell structure is possible. The inner ring of the cell ($d_0 \leq 0.7$) is supported by an MC-CDMA system. An OFDMA system with RRM for the two closest interfering cells handles the outer ring. For the case that OFDMA cannot be supported by an RRM, only MC-CDMA should be used in the whole cell.

The comparison between the two transmission schemes should be fair in terms of resource load and system dimensions. The OFDMA system can be seen as perfectly designed by using RRM. In contrast, MC-CDMA does not exploit its full design potential. With a detection scheme applying iterative decoding and soft-interference cancellation MAI can be almost eliminated [11] and a RRM can be also implemented

by using the $M&Q$ -modification [1]. The performance of MC-CDMA would consequently improve.

V. CONCLUSION

This paper handles two proposed transmission schemes for 4G systems, namely OFDMA and MC-CDMA. The simulations compare the error performance of these two in a cellular environment. The multi-cell scenario is described by a propagation model for the path loss and shadowing is taken into account. In case of the OFDMA system an idealized radio resource management is introduced.

The simulations show that MC-CDMA can outperform ordinary OFDMA in the case of varying resource loads. In the core of the cell, MC-CDMA exploits the whole sub-carrier diversity and outperforms OFDMA for resource loads smaller than $3/4$. The use of the radio resource management for OFDMA can highly enhance the OFDMA performance in the peripheral cell area and OFDMA surpasses the MC-CDMA performance.

To achieve maximum performance, a radial partitioning like onion rings can be used for the cell structure. The inner ring is served by MC-CDMA and the outer ring by OFDMA with a radio resource management.

ACKNOWLEDGMENT

This work has been partially performed in the framework of the IST project IST-2003-507581 WINNER, which is partly funded by the European Union.

REFERENCES

- [1] K. Fazel and S. Kaiser, *Multi-Carrier and Spread Spectrum Systems*. John Wiley and Sons, 2003.
- [2] H. Atarashi, N. Maeda, S. Abeta, and M. Sawahashi, "Broadband packet wireless access based on VSF-OFCDM and MC/DS-CDMA," in *Proceedings of the IEEE Int. Personal, Indoor and Mobile Radio Commun. (PIMRC 02)*, Portugal, September 2002, pp. 992–997.
- [3] A. Svensson, A. Ahlen, A. Brunstrom, T. Ottosson, and M. Sternad, "An OFDM based system proposal for 4G downlinks," in *Proceedings of the Int. Workshop on Multi-Carrier Spread-Spectrum & Related Topics (MC-SS 03)*, September 2003, pp. 15–22.
- [4] S. B. Weinstein and P. M. Ebert, "Data transmission by frequency division multiplexing using the discrete Fourier transform," *IEEE Transactions on Communications*, vol. COM-19, no. 15, pp. 628–634, October 1971.
- [5] S. Plass, A. Dammann, and S. Kaiser, "Analysis of coded OFDMA in a downlink multi-cell scenario," in *Proceedings of 9th Int. OFDM Workshop (InOwO 04)*, Dresden, Germany, September 2004.
- [6] J. G. Proakis, *Digital Communications*, 3rd ed. McGraw-Hill, 1995.
- [7] P. Hoeher, "A statistical discrete-time model for the WSSUS multipath channel," *IEEE Trans. Veh. Technol.*, vol. 41, pp. 461–468, November 1992.
- [8] G. D. Ott and A. Plitkins, "Urban path-loss characteristics at 820MHz," *IEEE Trans. Veh. Technol.*, vol. VT-27, pp. 189–197, November 1978.
- [9] S. Plass, S. Sand, and G. Auer, "Modeling and analysis of a cellular MC-CDMA downlink system," in *Proceedings of the IEEE Int. Personal, Indoor and Mobile Radio Communications (PIMRC 04)*, Barcelona, Spain, September 2004.
- [10] Y. Kishiyama, N. Maeda, K. Higuchi, H. Atarashi, and M. Sawahashi, "Experiments on throughput performance above 100-Mbps in forward link for VSF-OFCDM broadband packet wireless access," in *Proceedings IEEE Vehic. Technol. Conf. 2003-Fall (VTC'F 03)*, Orlando, USA, October 2003.
- [11] S. Kaiser and J. Hagenauer, "Multi-carrier CDMA with iterative decoding and soft-interference cancellation," in *Proceedings IEEE Global Telecommunications Conference (GLOBECOM 97)*, Phoenix, USA, November 1997, pp. 6–10.